J|A|C|S
ARTICLES
Published on Web 10/08/2004

Oscillation of Conductance in Molecular Junctions of Carbon Ladder Compounds

Tomofumi Tada, Daijiro Nozaki, Masakazu Kondo, Shinya Hamayama, and Kazunari Yoshizawa*

Contribution from the Institute for Materials Chemistry and Engineering, Kyushu University, Fukuoka 812-8581, Japan

Received December 16, 2003; E-mail: kazunari@ms.ifoc.kyushu-u.ac.jp

Abstract: The electrical conductances of dithiolates of polyacene (PA(*n*)DTs) and polyphenanthrene (PPh-(*n*)DTs), which are typical carbon ladder compounds, are calculated by means of the Landauer formulation combined with density functional theory, where *n* is the number of benzene rings involved. Surface Green function used in the Landauer formulation is calculated with the Slater−Koster parameters. Attention is turned to the wire-length dependence of the conductances of PA(*n*)DTs and PPh(*n*)DTs. The damping of conductance of PA(*n*)DTs is much smaller than that of PPh(*n*)DTs because of the small HOMO−LUMO gaps of PA(*n*)DTs. PA(*n*)DTs are thus good molecular wires for nanosized electronic devices. Conductance oscillation is found for both molecular wires when *n* is less than 7. The electrical conductance is enhanced in PA(*n*)DTs with even-numbered benzene rings, whereas it is enhanced in PPh(*n*)DTs with odd-numbered benzene rings. The observed conductance oscillation of PA(*n*)DTs and PPh(*n*)DTs is due to the oscillation of orbital energy and electron population. Other π-conjugated oligomers (polyacetylene-DT, oligo(thiophene)-DT, oligo(*meso*-*meso*-linked zinc(II) porphyrin-butadiynylene)-DT, oligo(*p*-phenylethynylene)-DT, and oligo-(*p*-phenylene)-DT) are also studied. In contrast to PA(*n*)DTs and PPh(*n*)DTs, the five molecular wires show ordinary exponential decays of conductance.

Introduction

Much interest in the electronic properties of carbon-based compounds has grown because of their technological development and applications in electrode materials. Theoretical studies have revealed that the electronic properties of carbon ladder oligomers significantly depend on their molecular size and edge structure.[1−6] One of the most important edge structures is "acene-edge type" and another is "phenanthrene-edge type" as shown in Chart 1. The two edge structures affect the electronic properties such as the HOMO−LUMO gaps: (I) in the acene-edge structure, the frontier orbitals are localized well at the edges, whereas in the phenanthrene-edge structure they are distributed over the molecule; (II) the HOMO−LUMO gaps of carbon ladder oligomers with the acene-edge type are much smaller than those with the phenanthrene-edge type. For example, the band gaps of polyacene and polyphenanthrene with

Chart 1

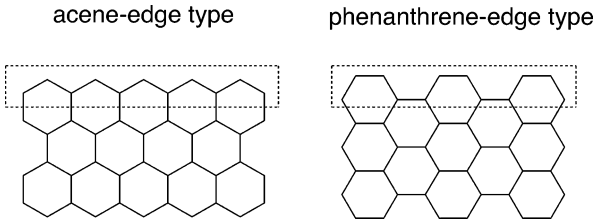

isodistant C−C bonds were calculated with the extended Hückel method to be 0.0 and ca. 1.8 eV, respectively.[6] Thus, polyacene is suitable for a highly conductive material. In fact, polyacene derivatives deposited on the SiO_2 layer show high on/off ratios ($> 10^4$) of current in field-effect transistors.[7] Pentacene, hexacene, and heptacene, which belong to a member of acene oligomers, are synthesized by means of the Diels−Alder reaction.[8] Unidirectional rows of pentacene molecules fabricated on Cu(110) surface were observed with the scanning tunneling microscope (STM) technique.[9] The highly ordered rows of pentacene are stable for temperatures up to 450 K and are useful as a template of nanosized circuits. Acene oligomers will thus play a role as building blocks of nanosized molecular devices. We focus on the electrical conductance of molecular junctions consisting of polyacene and polyphenanthrene in this study.

(1) (a) Hess, B. A., Jr.; Schaad, L. J. *J. Am. Chem. Soc.* **1971**, *93*, 305. (b) Hess, B. A., Jr.; Schaad, L. J. *J. Org. Chem.* **1971**, *36*, 3418.
(2) (a) Herndon, W. C. *Tetrahedron* **1973**, *29*, 3. (b) Herndon, W. C.; Ellzey, M. L. *J. Am. Chem. Soc.* **1974**, *96*, 6631. (c) Herndon, W. C. *J. Org. Chem.* **1975**, *40*, 3583. (d) Herndon, W. C. *J. Org. Chem.* **1981**, *46*, 2119. (e) Herndon, W. C. *Tetrahedron* **1982**, *38*, 1389.
(3) (a) Stein, S. E.; Brown, R. L. *Carbon* **1985**, *23*, 105. (b) Stein, S. E.; Brown, R. L. *J. Am. Chem. Soc.* **1987**, *109*, 3721. (c) Chen, R. H.; Kafafi, S. A.; Stein, S. E. *J. Am. Chem. Soc.* **1989**, *111*, 1418. (d) Stein, S. E.; Brown, R. L. *J. Am. Chem. Soc.* **1991**, *113*, 787. (e) Stein, S. E. *Acc. Chem. Res* **1991**, *24*, 350.
(4) Klimkâns, A.; Larsson, S. *Chem. Phys.* **1994**, *189*, 25.
(5) (a) Yamabe, T.; Yamashita, S.; Yamabe, H.; Fukui, K.; Tanaka, K. *Collect. Czech. Chem. Commun.* **1988**, *53*, 1881. (b) Yoshizawa, K.; Okahara, K.; Sato, T.; Tanaka, K.; Yamabe, T. *Carbon* **1994**, *32*, 1517.
(6) Yoshizawa, K.; Yahara, K.; Tanaka, K.; Yamabe, T. *J. Phys. Chem. B* **1998**, *102*, 498.
(7) Miao, Q.; Nguyen, T.-Q.; Someya, T.; Blanchet, G. B.; Nuckolls, C. *J. Am. Chem. Soc.* **2003**, *125*, 10284.
(8) Hopf, H. In *Classics in hydrocarbon chemistry*; Wiley-VCH: New York, 2000.
(9) Lukas, S.; Witte, G.; Wöll, Ch. *Phys. Rev. Lett.* **2002**, *88*, 028301.

10.1021/ja031736+ CCC: $27.50

Nanosized junctions consisting of molecular or atomic wires are prepared by means of STM,[10−14] atomic force microscope (AFM),[15−17] and break junction technique.[18−22] Conductance G of nanosized junctions is obtained from measured current−voltage responses. Sulfur atoms tend to make good bonding with gold atoms, and thereby various dithiolate species combined with gold electrodes have been characterized as molecular junctions.[10,11,14,19,20] In addition, the terminal sulfur atoms as alligator clips are able to promote the quantum transport through a π-conjugated molecule.[23] The understanding of the mechanism of quantum transport effects has been increased on the basis of theoretical investigations.[24] New prototypes of molecular devices for rectifiers,[25,26] switches,[27,28] logic gates,[29,30] and transistors[31] were proposed in theoretical studies. The exponential law of conductance ($G = G_m \exp[-\gamma L]$) is a useful guideline in preparing an efficient molecular wire, where G_m, γ, and L are, respectively, the contact conductance, the damping factor, and the molecular length.[32] A small damping factor ($\gamma = 0.0095$ Å^{-1}) and a large contact conductance ($G_m = 1.082\ G_0$) were theoretically predicted in tape-porphyrin molecular wires,[33] where G_0 is the quantum unit of conductance ($2e^2/h$). In contrast to molecular wires, the electrical conductance of atomic wires[34] does not necessarily show the exponential decay as a function of the wire length. Various groups have predicted conductance oscillation in atomic wires (Na atomic wires[35−37] and C atomic wires[38−41]) from theoretical calculations. The conductance of a wire with odd-numbered atoms is nearly equal to the quantum unit of conductance ($2e^2/h$) while the conductance of a wire with even-numbered atoms is smaller than the unit. Palacios and co-workers[41] reported using first-principles calculations of the Landauer formalism[42] for electrical transmission that the even−odd periodicity of conductance is reversed for junctions composed of short C atomic wires and Al electrodes. The parity oscillation of conductance was recently observed in the atomic wires composed of Au, Pt, or Ir atoms.[22] A novel junction composed of Au atomic wires and Cu(II) phthalocyanine was prepared on the NiAl(110) surface (Chart 2).[43] This type of junction will be useful in the construction of nanosized devices because of its small size and the well-defined structure, and thus the wire-length dependence of electrical conductance in atomic and molecular wires is an important issue for the design of effective nanostructures.

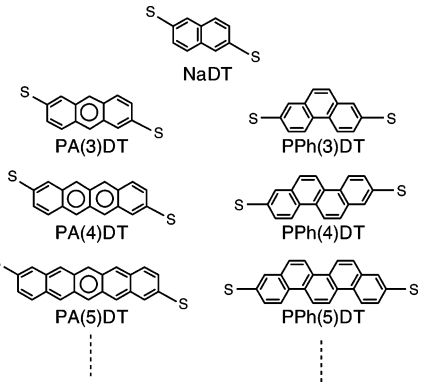

Figure 1. Polyacene dithiolates, PA(n)DTs, and polyphenanthrene dithiolates, PPh(n)DTs, in which n is the number of benzene rings involved. The naphthalene dithiolate (NaDT) molecule is identical with PA(2)DT and PPh(2)DT.

Chart 2

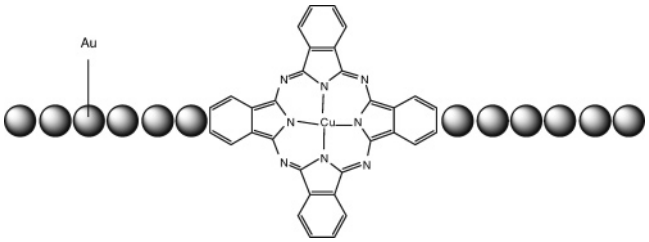

In this paper, we present the electrical conductances of polyacene dithiolates (PA(n)DTs) and polyphenanthrene dithiolates (PPh(n)DTs) shown in Figure 1 on the basis of the Landauer formalism combined with density functional theory (DFT).[44,45] We predict that the conductances of PA(n)DTs and

(10) Bumm, L. A.; Arnold, J. J.; Dunbar, T. D.; Allara, D. L.; Weiss, P. S. *J. Phys. Chem B* **1999**, *103*, 8122.
(11) Gittins, D. I.; Bethell, D.; Schiffrin, D. J.; Nichols, R. J. *Nature* **2000**, *408*, 67.
(12) Toerker, M.; Fritz, T.; Proehl, H.; Gutierrez, R.; Grossmann, F.; Schmidt, R. *Phys. Rev. B* **2002**, *65*, 245422.
(13) Xu, B.; Tao, N. J. *Science* **2003**, *301*, 1221.
(14) Kasibhatla, B. S. T.; Labonté, A. P.; Zahid, F.; Reifenberger, R. G.; Datta, S.; Kubiak, C. P. *J. Phys. Chem. B* **2003**, *107*, 12378.
(15) Cui, X. D.; Primak, A.; Zarate, X.; Tomfohr, J.; Sankey, O. F.; Moore, A. L.; Moore, T. A.; Gust, D.; Harris, G.; Lindsay, S. M. *Science* **2001**, *294*, 571.
(16) Wold, D. J.; Haag, R.; Rampi, M. A.; Frisbie, C. D. *J. Phys. Chem. B* **2002**, *106*, 2813.
(17) Ishida, T.; Mizutani, W.; Aya, Y.; Ogiso, H.; Sasaki, S.; Tokumoto, H. *J. Phys. Chem. B*, **2002**, *106*, 5886.
(18) Reed, M. A.; Zhou, C.; Muller, C. J.; Burgin, T. P.; Tour, J. M. *Science* **1997**, *278*, 252.
(19) Kergueris, C.; Bourgoin, J.-P.; Palacin, S.; Esteve, D.; Urbina, C.; Magoga, M.; Joachim, C. *Phys. Rev. B* **1999**, *59*, 12505.
(20) Reichert, J.; Ochs, R.; Beckmann, D.; Weber, H. B.; Mayor, M.; van Löhneysen, H. *Phys. Rev. Lett.* **2002**, *88*, 176804.
(21) Smit, R. H. M.; Noat, Y.; Untiedt, C.; Lang, N. D.; van Hemert, M. C.; van Ruitenbeek, J. M. *Nature* **2002**, *419*, 906.
(22) Smit, R. H. M.; Untiedt, C.; Rubio-Bollinger, G.; Segers, R. C.; van Ruitenbeek, J. M. *Phys. Rev. Lett.* **2003**, *91*, 076805.
(23) Our preliminary calculations demonstrated that a π-conjugated molecule with S−Au connections has a higher conductance by 2 orders of magnitude than that with direct C−Au connections.
(24) See for example: (a) Samanta, M. P.; Tian, W.; Datta, S.; Henderson, J. I.; Kubiak, C. P. *Phys. Rev. B* **1996**, *53*, R7626. (b) Mujica, V.; Kemp, M.; Roitberg, A.; Ratner, M. *J. Chem. Phys.* **1996**, *104*, 7296. (c) Emberly, E. G.; Kirczenow, G. *Phys. Rev. B* **1998**, *58*, 10911. (d) Derosa, P. A.; Seminario, J. M. *J. Phys. Chem. B* **2001**, *105*, 471. (e) Lang, N. D.; Avouris, Ph. *Phys. Rev. B* **2001**, *64*, 125323. (f) Nakanishi, S.; Tsukada, M. *Phys. Rev. Lett.* **2001**, *87*, 126801. (g) Brandbyge, M.; Mozos, J.-L.; Ordejón, P.; Taylor, J.; Stokbro, K. *Phys. Rev. B* **2002**, *65*, 165401. (h) Nitzan, A.; Ratner, M. A. *Science*, **2003**, *300*, 1384, and references therein.
(25) (a) Seminario, J. M.; Zacarias, A. G.; Tour, J. M. *J. Am. Chem. Soc.* **2000**, *122*, 3015. (b) Derosa, P. A.; Guda, S.; Seminario, J. M. *J. Am. Chem. Soc.* **2003**, *125*, 14240.
(26) Stokbro, K.; Taylor, J.; Brandbyge, M. *J. Am. Chem. Soc.* **2003**, *125*, 3674.
(27) Taylor, J.; Guo, H.; Wang, J. *Phys. Rev. B* **2001**, *63*, 121104.
(28) Baer, R.; Neuhauser, D. *J. Am. Chem. Soc.* **2002**, *124*, 4200.
(29) (a) Ami, S.; Joachim, C. *Phys. Rev. B* **2002**, *65*, 155419. (b) Ami, S.; Hliwa, M.; Joachim, C. *Chem. Phys. Lett.* **2003**, *367*, 662.
(30) Baer, R.; Neuhauser, D. *Chem. Phys.* **2002**, *281*, 353.
(31) Alavi, S.; Larade, B.; Taylor, J.; Guo, H.; Seideman, T. *Chem. Phys.* **2002**, *281*, 293.
(32) Magoga, M.; Joachim, C. *Phys. Rev. B* **1997**, *56*, 4722.
(33) (a) Tagami, K.; Tsukada, M.; Matsumoto, T.; Kawai, T. *Phys. Rev. B* **2003**, *67*, 245324. (b) Tagami, K.; Tsukada, M. *Jpn. J. Appl. Phys.* **2003**, *42*, 3606.
(34) For example, theoretical studies of transport effects in atomic wires were reported in (a) Schreiber, M.; Maschke, K. *Z. Phys. B − Condensed Matter* **1991**, *85*, 123. (b) Burmeister, G.; Maschke, K.; Schreiber, M. *Phys. Rev. B* **1993**, *47*, 7095. (c) Ozpineci, A.; Ciraci, S. *Phys. Rev. B* **2001**, *63*, 125415. (d) Bai, Z.-M.; Wang, Y.-R.; Ge, M.-L. *J. Phys. A* **2001**, *34*, 1595.
(35) Lang, N. D. *Phys. Rev. Lett.* **1997**, *79*, 1357.
(36) Sim, H.-S.; Lee, H.-W.; Chang, K. J. *Phys. Rev. Lett.* **2001**, *87*, 096803.
(37) Havu, P.; Torsti, T.; Puska, M. J.; Nieminen, R. M. *Phys. Rev. B* **2002**, *66*, 075401.
(38) Lang, N. D.; Avouris, Ph. *Phys. Rev. Lett.* **1998**, *81*, 3515.
(39) Lang, N. D.; Avouris, Ph. *Phys. Rev. Lett.* **2000**, *84*, 358.
(40) Larade, B.; Taylor, J.; Mehrez, H.; Guo, H. *Phys. Rev. B* **2001**, *64*, 075420.
(41) Palacios, J. J.; Pérez-Jiménez, A. J.; Louis, E.; SanFabián, E.; Vergés, J. A. *Phys. Rev. B* **2002**, *66*, 035322.
(42) Datta, S. *Electronic Transport in Mesoscopic Systems*; Cambridge University Press: Cambridge, 1995.
(43) Nazin, G. V.; Qiu, X. H.; Ho, W. *Science* **2003**, *302*, 77.

PPh(n)DTs oscillate as a function of the number of benzene rings involved. The even−odd periodicity in the conductance oscillation of PA(n)DTs is different from that of PPh(n)DTs. The conductance is enhanced in PA(n)DTs involving even-numbered benzene rings, whereas it is enhanced in PPh(n)DTs with odd-numbered benzene rings. We analyze the conductance oscillation by looking at the frontier orbitals of these dithiolate molecules.

2. Methodology

On the basis of the Landauer formalism, the electrical conductance G of a molecular junction consisting of an insulating molecule (I) and two metallic electrodes (M), M−I−M junction, at low temperature is written as follows[42]

$$G = \frac{2e^2}{h} T(E_F) \tag{1}$$

where $T(E_F)$ is the transmission function at the Fermi level E_F. We can calculate the transmission function from eq 2

$$T(E) = \mathrm{Tr}[\Gamma_L(E)\mathbf{G}^R(E)\Gamma_R(E)\mathbf{G}^A(E)] \tag{2}$$

where $\mathbf{G}^{R(A)}$ is the matrix of retarded (advanced) Green function of the molecule; $\Gamma_{L(R)}$ is written in terms of the self-energy Σ as $i[\Sigma^R_{L(R)} - \Sigma^A_{L(R)}]$. The self-energy matrixes for the left and right side electrodes are $\Sigma_L^{R/A} = \tau_L^+ \mathbf{g}_L^{R/A} \tau_L$ and $\Sigma_R^{R/A} = \tau_R^+ \mathbf{g}_R^{R/A} \tau_R$, respectively. $\mathbf{g}_L{}^{R/A}$ and $\mathbf{g}_R{}^{R/A}$ are the Green functions of the left and right side electrodes uncoupled with the molecule, respectively, and $\tau_{L(R)}$ is the matrix of hopping integrals between the left (right) electrode and the molecule. We take only the nearest neighbor interactions between the electrodes and the molecule into account because other interactions such as the second and third neighbor interactions are small. In this formalism, the retarded and advanced Green function $\mathbf{G}^{R/A}$ in the molecular part is given as eq 3

$$\mathbf{G}^{R/A}(E) = [\mathbf{I} - \mathbf{G}^{(0)R/A}(E)\Sigma^{R/A}(E)]^{-1}\mathbf{G}^{(0)R/A}(E) \tag{3}$$

where $\mathbf{I}$ is the unit matrix and $\mathbf{G}^{(0)R/A}$ is the Green function of the molecule (the zeroth order Green function). This equation is easily derived from the Dyson equation, $\mathbf{G} = \mathbf{G}^{(0)} + \mathbf{G}^{(0)}\Sigma\mathbf{G}$. The matrix elements of $\mathbf{G}^{(0)R/A}$ can be written in terms of MO coefficients C's as follows

$$[\mathbf{G}^{(0)R/A}(E)]_{\alpha\beta} = \sum_m \frac{C_{m\alpha}C_{m\beta}}{E - \epsilon_m \pm i\eta} \tag{4}$$

$C_{m\alpha}$ denotes the mth MO coefficient at atomic orbital α, ϵ_m is the mth MO energy of the molecule, and η is an infinitesimal constant. The expression for $\mathbf{G}^{(0)}$s in eq 4 is useful in the understanding of correlations between electrical conductance and MOs. We have analyzed the conductances of molecular wires (e.g., nanosized graphite sheets,[46] a DNA molecule,[47] and benzene 1,4-dithiole (BDT)[48]) by looking at their MOs. Although the present formalism using the MO expansion looks different from the one often employed in the calculation of the Green functions,[49] we confirmed that a computed conductance of BDT with this methodology (0.004 G_0) is in good agreement with the values previously computed[24d] and observed[50] (approximately 0.01 G_0).

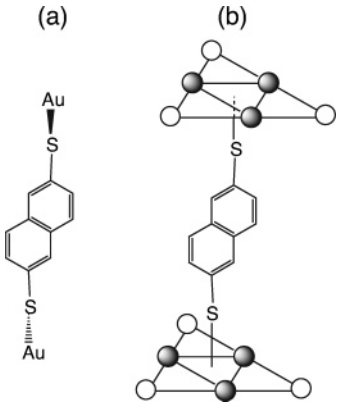

Figure 2. (a) NaDT coupled with two gold atoms. (b) NaDT sandwiched by two Au(111) surfaces. The shaded circles are the gold atoms included in the calculations of conductance. The nearest Au−Au distances are 2.88 Å, the bond length of bulk gold.

3. Computational Details

Many theoretical studies show that the calculation of molecules including part of electrodes provides reasonable MO levels relative to the Fermi level of the electrodes. For example, Heurich et al.[51] suggested that the addition of one gold atom to each side of a molecular wire ensures qualitative description of the charge transfer between gold electrodes and the molecular wire. A molecular wire with additional gold atoms is in general called "extended molecule". Thus, we calculated the electronic structures of PA(n)DTs and PPh(n)DTs with additional gold atoms bonded with the terminal sulfur atoms. Figure 2(a) shows the conformation of naphthalene-dithiolate (NaDT) coupled with two gold atoms, the two gold atoms being located out of the NaDT plane. We employed the B3LYP method,[52] which consists of the Slater exchange, the Hartree−Fock exchange, the exchange functional of Becke,[53] the correlation functional of Lee, Yang, and Parr (LYP),[54] and the correlation functional of Vosko, Wilk, and Nusair,[55] incorporated in the Gaussian 98 code[56] for geometry optimizations of the extended molecules. We used the LANL2DZ basis set[57,58] for all atoms.

(44) Hohenberg, P.; Kohn, W. *Phys. Rev.* **1964**, *136*, B864.
(45) Kohn, W.; Sham, L. J. *Phys. Rev.* **1965**, *140*, A1133.
(46) (a) Tada, T.; Yoshizawa, K. *ChemPhysChem* **2002**, *3*, 1035. (b) Tada, T.; Yoshizawa, K. *J. Phys. Chem. B* **2003**, *107*, 8789.
(47) Tada, T.; Kondo, M.; Yoshizawa, K. *ChemPhysChem* **2003**, *4*, 1256.
(48) Kondo, M.; Tada, T.; Yoshizawa, K. *J. Phys. Chem. A*, in press.
(49) The Green functions are often calculated by using the following relation: $\mathbf{G}(E) = [E\mathbf{1} - \mathbf{H} - \Sigma]^{-1}$, where $\mathbf{H}$ is the Hamiltonian matrix of a molecule and Σ is the self-energy matrix accounting for the interactions between a molecule and electrodes. See for example: (a) Palacios, J. J.; Pérez-Jiménez, A. J.; Louis, E.; Vergés, J. A. *Phys. Rev. B* **2001**, *64*, 115411. (b) Seminario, J. M.; Zacarias, A. G.; Derosa, P. A. *J. Chem. Phys.* **2002**, *116*, 1671.
(50) Xiao, X.; Xu, B.; Tao, N. J. *Nano Lett.* **2004**, *4*, 267.
(51) Heurich, J.; Cuevas, J. C.; Wenzel, W.; Schön, G. *Phys. Rev. Lett.* **2002**, *88*, 256803.
(52) Becke, A. D. *J. Chem. Phys.* **1993**, *98*, 5648.
(53) Becke, A. D.; Roussel, M. R. *Phys. Rev. A* **1989**, *39*, 3761.
(54) Lee, C.; Yang, W.; Parr, R. G. *Phys. Rev. B* **1988**, *37*, 785.
(55) Vosko, S. H.; Wilk, L.; Nusair, M. *Can. J. Chem.* **1980**, *58*, 1200.
(56) Frisch, M. J.; Trucks, G. W.; Schlegel, H. B.; Scuseria, G. E.; Robb, M. A.; Cheeseman, J. R.; Zakrzewski, V. G.; Montgomery, J. A., Jr.; Stratmann, R. E.; Burant, J. C.; Dapprich, S.; Millam, J. M.; Daniels, A. D.; Kudin, K. N.; Strain, M. C.; Farkas, O.; Tomasi, J.; Barone, V.; Cossi, M.; Cammi, R.; Mennucci, B.; Pomelli, C.; Adamo, C.; Clifford, S.; Ochterski, J.; Petersson, G. A.; Ayala, P. Y.; Cui, Q.; Morokuma, K.; Malick, D. K.; Rabuck, A. D.; Raghavachari, K.; Foresman, J. B.; Cioslowski, J.; Ortiz, J. V.; Stefanov, B. B.; Liu, G.; Liashenko, A.; Piskorz, P.; Komaromi, I.; Gomperts, R.; Martin, R. L.; Fox, D. J.; Keith, T.; Al-Laham, M. A.; Peng, C. Y.; Nanayakkara, A.; Gonzalez, C.; Challacombe, M.; Gill, P. M. W.; Johnson, B.; Chen, W.; Wong, M. W.; Andres, J. L.; Head-Gordon, M.; Replogle, E. S.; Pople, J. A. *Gaussian 98*; Gaussian Inc.: Pittsburgh, PA, 1998.
(57) Dunning, T. H., Jr.; Hay, P. J. In *Modern Theoretical Chemistry*; Schaefer, H. F., III, Ed.; Plenum: New York, 1976; Vol. 3, p 1.
(58) (a)Wadt, W. R.; Hay, P. J. *J. Chem. Phys.* **1985**, *82*, 284. (b) Hay, P. J.; Wadt, W. R. *J. Chem. Phys.* **1985**, *82*, 299.

Table 1. Orbital Energies of the Frontier Orbitals and Mulliken Charges for Au−PA(7)DT−Au, Au_3-PA(7)DT−Au_3, and Au_9−PA(7)DT−Au_9 Calculated at the B3LYP/LANL2DZ Level

	Au–PA(7)DT–Au	Au_3–PA(7)DT–Au_3	Au_9–PA(7)DT–Au_9
	orbital energy (eV)		
LUMO+6	−0.44	−1.26	−3.25[b]
LUMO+5	−1.00	−2.23	−3.50[c]
LUMO+4	−1.18	−3.13	−3.51[c]
LUMO+3	−2.17	−3.32	−3.53[c]
LUMO+2	−3.19	−3.32	−3.53[c]
LUMO+1	−3.55	−3.34	−3.91[c]
LUMO	−3.65[b]	−3.52[b]	−3.92[c]
HOMO	−4.82[a]	−4.85[a]	−4.50[c]
HOMO-1	−5.75	−5.52	−4.52[c]
HOMO-2	−6.34	−5.52	−4.72[a]
	Mulliken charges		
PA(7)DT	+0.16	−0.10	−0.12
Au (cluster)[d]	−0.08	+0.05	+0.06

[a] The phase of the HOMO of Au−PA(7)DT−Au is similar to that of the HOMO of Au_3−PA(7)DT−Au_3 and the HOMO-2 of Au_9−PA(7)DT−Au_9. [b] The phase of the LUMO of Au−PA(7)DT−Au is similar to that of the LUMO of Au_3−PA(7)DT−Au_3 and the LUMO+6 of Au_9−PA(7)DT−Au_9. [c] The amplitudes of the HOMO-1 to the LUMO+5 of Au_9−PA(7)DT−Au_9 are localized at one of the Au_9 clusters. That is, the symmetry of the MOs is broken. [d] Mulliken charges of the Au atoms in Au−PA(7)DT−Au, the Au_3 clusters in Au_3−PA(7)DT−Au_3, and the Au_9 clusters in Au_9−PA(7)DT−Au_9.

Optimized geometries of PA(*n*)DTs and PPh(*n*)DTs are shown in Figures S1 and S2 of the Supporting Information. We obtained the zeroth order Green function matrix elements of the extended molecules from eq 4 using the MO coefficients and the orbital energies calculated at the B3LYP/LANL2DZ level.

To take the molecule-electrode interactions into account appropriately, we considered the dithiolate molecules intercalated between two Au(111) surfaces. Figure 2(b) shows the conformation of NaDT and the Au(111) surfaces, in which we adopted the hopping integrals between the AOs of the gold and sulfur atoms as the molecule-electrode coupling elements in τ's. The sulfur atoms are placed on a 3-fold hollow site on the Au(111) surfaces as shown in Figure 2(b), in which the Au−S bond lengths are set to be 2.40 Å.[59] According to Seminario's study,[60] the hollow site is the most favorable for binding in view of the binding energies of Au_n−S systems. We obtained the matrix elements of τ's with the extended Hückel method.[61] The Green function of the Au(111) surface were calculated from the decimation technique[62,63] using the Slater−Koster two-center parameters;[64,65] the Hamiltonian matrix elements given in Table 1 of ref 64 were used.

4. Results and Discussion

4.1 Location of the Fermi Level. How we define the location of the Fermi level E_F is important in the calculation of the conductance of molecular wires. The work function of Au (−5.31 eV)[66] has been used in many theoretical studies as the Fermi level of gold electrodes. Let us first consider a reasonable determination of the Fermi level in PA(*n*)DTs. Figure 3 shows orbital energies of PA(*n*)DTs coupled with two gold atoms, indicating that the HOMO−LUMO gaps are decreased rapidly with an increase in molecular length. If E_F is set to be the work function of Au, electrons occupied at the HOMOs of PA(*n*)-DTs for $n = 5$ to 9 will be transferred to the electrodes, so that PA(*n*)DTs for $n = 5$ to 9 will be positively charged. To consider a better location of the Fermi level, we performed a DFT calculation of the Au_{20} cluster with T_d symmetry at the B3LYP/LANL2DZ level and confirmed that the midgap of the Au_{20} cluster is −4.94 eV. When we use the midgap as the Fermi level, the charge transfer to the electrodes will also occur in PA(*n*)DTs for $n = 7$ to 9. Thus, to clarify whether the charge transfer is realistic or not, we calculated the electronic states of the Au_3−PA(7)DT−Au_3 and Au_9−PA(7)DT−Au_9 systems in Figure 4. Table 1 lists computed energies of the frontier orbitals of Au−PA(7)DT−Au, Au_3−PA(7)DT−Au_3, and Au_9−PA(7)-DT−Au_9. The HOMO of Au−PA(7)DT−Au is delocalized in

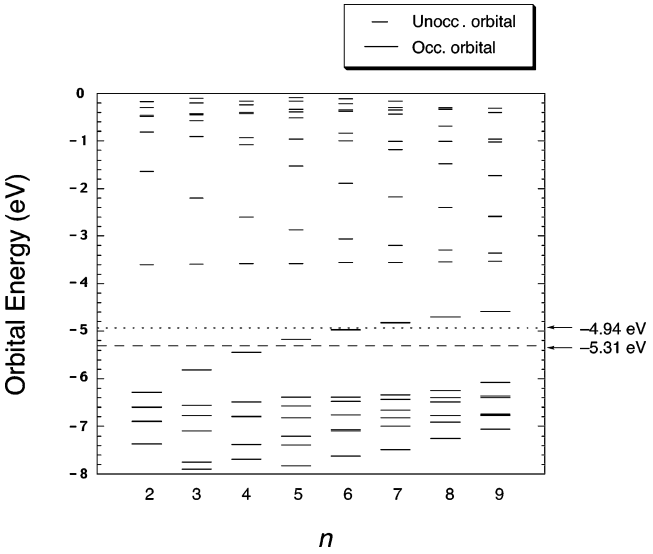

Figure 3. Energies of the frontier orbitals of PA(*n*)DTs ($n = 2$ to 9) coupled with two Au atoms calculated. The long and short bars mean occupied and unoccupied MOs, respectively. The work function of gold (−5.31 eV) and the midgap of the Au_{20} cluster (−4.94 eV) are indicated by the broken and the dotted lines, respectively.

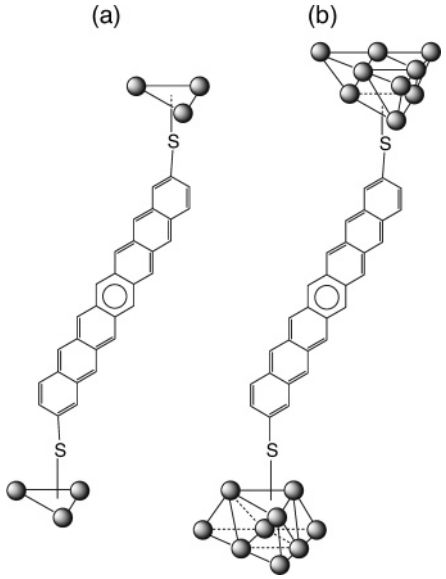

Figure 4. Conformations of (a) PA(7)DT coupled with two Au_3 clusters and (b) PA(7)DT with two Au_9 clusters. The nearest neighbor distances between gold atoms are 2.88 Å.

(59) Optimized Au−S bond lengths of PPh(*n*)DTs and PA(*n*)DTs with additional two gold atoms are about 2.4 Å at B3LYP/LNAL2DZ level of theory as shown in Figures 1S and 2S of the Supporting Information.
(60) Seminario, J. M.; Zacarias, A. G.; Tour, J. M. *J. Am. Chem. Soc.* **1999**, *121*, 411.
(61) Hoffmann, R. *J. Chem. Phys.* **1963**, *39*, 1397.
(62) Guinea, F.; Tejedor, C.; Flores, F.; Louis, E. *Phys. Rev. B* **1983**, *28*, 4397.
(63) López-Sancho, M. P.; López-Sancho, J. M.; Rubio, J. *J. Phys. F* **1985**, *15*, 851.
(64) Slater, J. C.; Koster, G. F. *Phys. Rev.* **1954**, *94*, 1498.
(65) Papaconstantopoulos, D. A. In *Handbook of the Band Structure of Elemental Solids*; Plenum: New York, 1986.
(66) *CRC Handbook of Chemistry and Physics*, 81th ed.; Lide, D. R., Ed.; CRC Press: Boca Raton, FL, 2000; p 12-130.

Chart 3

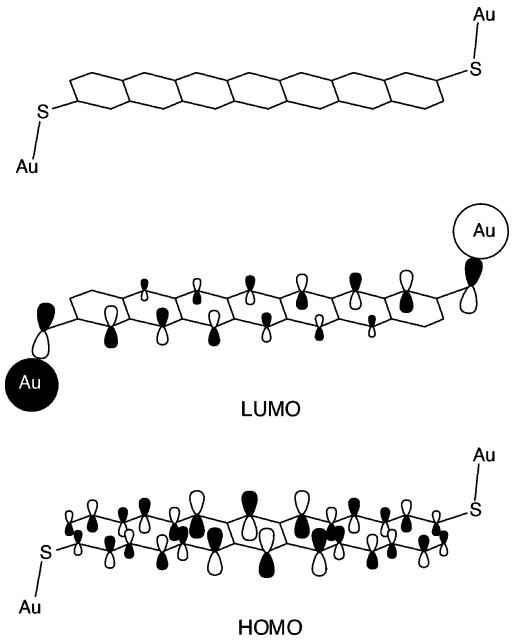

PA(7)DT, whereas the LUMO is localized at the sulfur and gold atoms, as depicted in Chart 3. Table 1 also lists computed Mulliken charges, demonstrating that the charge transfer from PA(7)DT to the Au clusters is very small. We can conclude that the spontaneous charge transfer of two electrons from PA(7)DT to the electrodes will not occur. Therefore, it is reasonable to consider the Fermi level to be located between the HOMO and LUMO of Au−PA(7)DT−Au. The midgap of Au−PA(7)DT−Au is −4.24 eV, and the level is close to the midgap of Au_9−PA(7)DT−Au_9 (−4.21 eV). Thus, we determined to set the Fermi level at the midgap for the extended molecules considered in the present study. We confirmed that the consideration given above from B3LYP/LANL2DZ calculations is not affected even when we use the B3PW91 functional[52,67] with the LANL2DZ basis set.

4.2 Conductance Oscillation in PA(*n*)DTs and PPh(*n*)DTs. Let us next consider the wire-length dependence of the conductances of PA(*n*)DTs and PPh(*n*)DTs. Figure 5(a) shows computed conductances *G*s of PA(*n*)DTs and PPh(*n*)DTs, where $n = 2\sim9$, at the B3LYP/LANL2DZ level of theory. When *n* is less than 7, the conductances of the two series oscillate as a function of the number of benzene rings involved. The conductance of PA(*n*)DT is enhanced when *n* is even, while that of PPh(*n*)DT is enhanced when *n* is odd. The conductance oscillation was observed in the hollow-site connection as well as in the other type connections, as summarized in Table 2. Although the conductance for the on-top connection is smaller than those for the hollow- and bridge-site connections, the parity of the oscillation is essentially identical in these connections. The conductance oscillation is also obtained from B3PW91/LANL2DZ calculations, as shown in Table 3. A previous study based on the Landauer formalism predicted conductance oscillation in the molecular wires composed of stilbene (1,2-diphenylethylene) and two alkene chains.[68] Thus, conductance oscillation should occur not only in atomic wires but also in molecular wires in general. To investigate whether other conjugated oligomers show the conductance oscillation, we calculated the electrical conductances of (A) polyacetylene-dithiolate, (B) oligo(thiophene)-dithiolate, (C) oligo(*meso-meso*-linked zinc(II) porphyrin-butadiynylene)-dithiolate, (D) oligo(*p*-phenylethynylene)-dithiolate, and (E) oligo(*p*-phenylene)-dithiolate shown in Figure 6. In contrast to PA(*n*)DT and PPh(*n*)DT, computed conductances of the five molecular wires do not oscillate, the decay of the conductances obeying the exponential law of *G* given as follows[32]

$$G = G_m e^{-\gamma L} \tag{5}$$

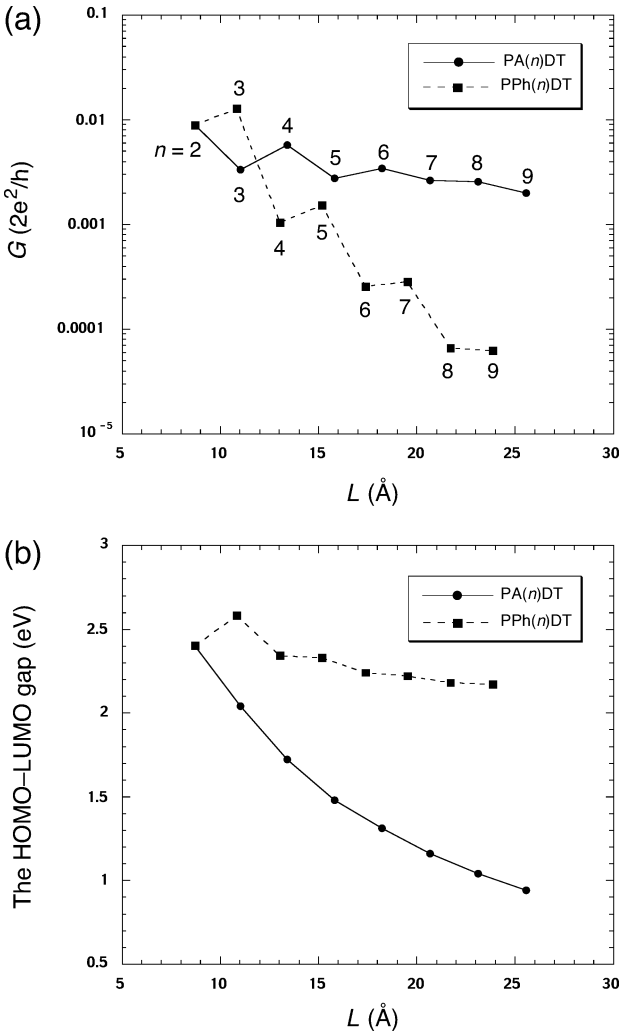

Figure 5. (a) Computed electrical conductance of PA(*n*)DTs and PPh(*n*)DTs ($n = 2$ to 9) and (b) HOMO−LUMO gaps of PA(*n*)DTs and PPh(*n*)DTs ($n = 2$ to 9). *L* is the length of the molecular wires, the distance between the two sulfur atoms.

Table 2. Computed Conductances of PA(*n*)DTs Connected at the Bridge and On-Top Sites of Au(111) Surface

	conductance ($2e^2/h$)	
n	bridge	on-top
2	0.0069	0.0003
3	0.0023	0.0005
4	0.0042	0.0010
5	0.0022	0.0005
6	0.0024	0.0008
7	0.0017	0.0006

(67) Perdew, J. P.; Chevary, J. A.; Vosko, S. H.; Jackson, K. A.; Pederson, M. R.; Singh, D. J.; Fiolhais, C. *Phys. Rev. B* **1992**, *46*, 6671.
(68) Gutiérrez, R.; Grossmann, F.; Schmidt, R. *ChemPhysChem* **2003**, *4*, 1252.

Table 3. Computed Conductances of PA(*n*)DTs at the B3LYP/LANL2DZ and B3PW91/LANL2DZ Levels[a]

	conductance ($2e^2/h$)	
n	B3LYP/LANL2DZ	B3PW91/LANL2DZ[a]
2	0.0089	0.0062
3	0.0029	0.0021
4	0.0057	0.0045
5	0.0027	0.0017
6	0.0034	0.0022
7	0.0026	0.0015

[a] The connection site between PA(n)DTs and gold electrodes is the hollow site. [b] Geometries of PA(n)DTs were optimized with B3PW91/LANL2DZ.

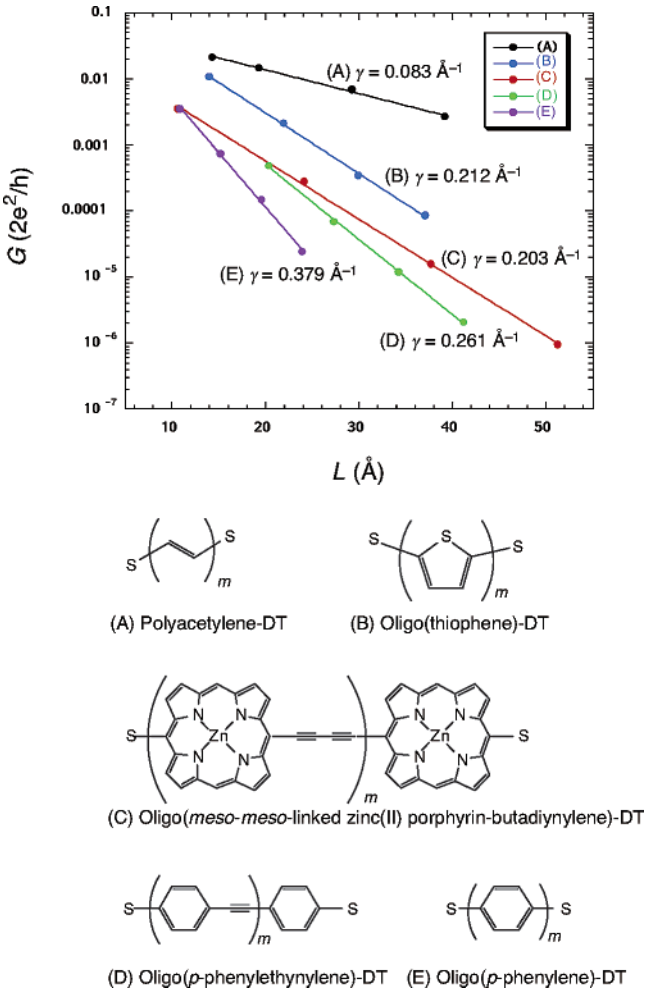

Figure 6. Wire-length dependence of the conductance for typical π-conjugated oligomers.

The damping factor γ is a feature of the molecular wires themselves, whereas the contact conductance G_m depends on the adsorption site between the wire ends and the surfaces of the electrodes. Figure 6 also shows calculated damping factors of the five oligomers. Magoga and Joachim[32] reported using the extended Hückel MO method that γ 's of polyacetylene, oligo(thiophene), oligo(*p*-phenylethynylene), and oligo(*p*-phenylene) are 0.187, 0.329, 0.278, and 0.281, respectively. Our γ's are consistent with these values. The damping factors of PA(*n*)DT and PPh(*n*)DT can be obtained for even- and odd-numbered benzene rings independently; computed γ's of PA(2*m*)DT and PA(2*m*+1)DT are 0.089 and 0.032 Å^{-1}, and γ's of PPh(2*m*)DT and PPh(2*m*+1)DT are 0.371 and 0.406 Å^{-1}, respectively. The damping factors of PA(2*m*)DT and PA(2*m*+1)DT are much smaller than those of PPh(2*m*)DT and PPh(2*m*+1)DT. The significant difference derives from the difference of the HOMO−LUMO gaps (Figure 5b). The HOMO−LUMO gaps of PA(*n*)DT decrease with an increase in wire length, whereas those of PPh(*n*)DT do not depend on wire length and they are larger than those of PA(*n*)DTs. Since, in general, the electron populations of the terminal sulfur atoms in a delocalized MO become small in longer wires, the conductance decays exponentially even when the HOMO−LUMO gaps are nearly constant like in PPh(*n*)DT. However, when the HOMO−LUMO gaps decrease rapidly with an increase in wire length, the contributions from the frontier orbitals in the zeroth order Green function (eq 4) are significant, and thereby the exponential decay is effectively weakened in PA(*n*)DT. In particular, the small damping factor of PA(2*m*+1)DT (0.032 Å^{-1}) means that the conductance hardly decays even in longer wires. Therefore polyacene dithiolates are good molecular wires in nanosized devices. The damping factors of PA(2*m*+1)DTs and PPh(2*m*+1)DTs are the small and large limits, respectively.

4.3 Analysis of the Conductance Oscillation. Finally, let us analyze the oscillation of conductance on the basis of the frontier orbitals. As shown in eq 4, the zeroth order Green function depends on MO coefficients and orbital energies. Since the Fermi level is located at the midgaps of the extended molecules coupled with two gold atoms, the frontier orbitals (the HOMO, LUMO, and other MOs in the vicinity of the Fermi level) play a significant role in the zeroth order Green function. We therefore think that the conductance oscillation should correlate with the populations and energies of the frontier orbitals on the basis of the concept of MO interactions[69,70] because eq 4 and second-order perturbation energies have similar forms. We previously derived an interesting relationship between the frontier orbitals and the conductance of molecular junctions of nano carbons and demonstrated that the orbital amplitudes and phases of the frontier orbitals are useful to predict effective quantum transport.[46] Gutiérrez and co-workers[68] also attributed the conductance oscillation in a molecular wire to oscillatory behavior of electron populations of the frontier orbitals.

We focus our attention on PPh(*n*)DTs and PA(*n*)DTs for $n = 2$ to 7, in which the conductance oscillation is obtained. To investigate how frontier orbitals dominate the conductance oscillation, we restricted the summation in eq 4 to some frontier orbitals to evaluate the transmission functions. We considered three types of summations as follows: (i) the HOMO and the LUMO, (ii) the HOMO-1 to the LUMO+1, and (iii) the HOMO-2 to the LUMO+2. Figure 7 shows transmission functions $T^f(E_F)$s calculated only from the frontier orbitals of PPh(*n*)DTs. Although we obtained the conductance oscillation by taking the HOMO and LUMO into account as shown in Figure 7a, the parity of the oscillation is not consistent with that of Figure 5a. The summation from the HOMO-1 to the LUMO+1 does not lead to the oscillation of conductance (Figure 7b). On the other hand, $T^f(E_F)$s computed with the summation from the HOMO-2 to the LUMO+2 oscillate with the even−odd parity corresponding with that of the conductance oscillation of PPh(*n*)DTs (Figure 7c).[71] That is, an important

(69) Fukui, K. *Angew. Chem., Int. Ed. Engl.* **1982**, *21*, 801 (Nobel Lecture).
(70) Hoffmann, R. *Angew. Chem., Int. Ed. Engl.* **1982**, *21*, 711 (Nobel Lecture).
(71) For PPh(6)DT and PPh(7)DT, the transmission functions calculated from the HOMO-3 to the LUMO+2 are shown in Figure 7(c).

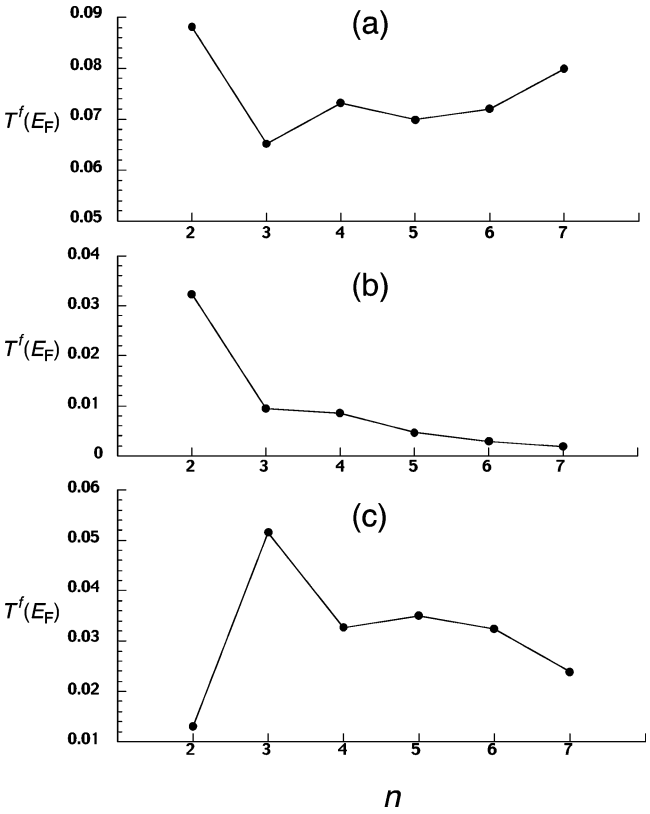

Figure 7. Transmission functions calculated only from (a) the HOMO and LUMO, (b) the HOMO-1 to the LUMO+1, and (c) the HOMO-2 to the LUMO+2 of PPh(*n*)DTs.

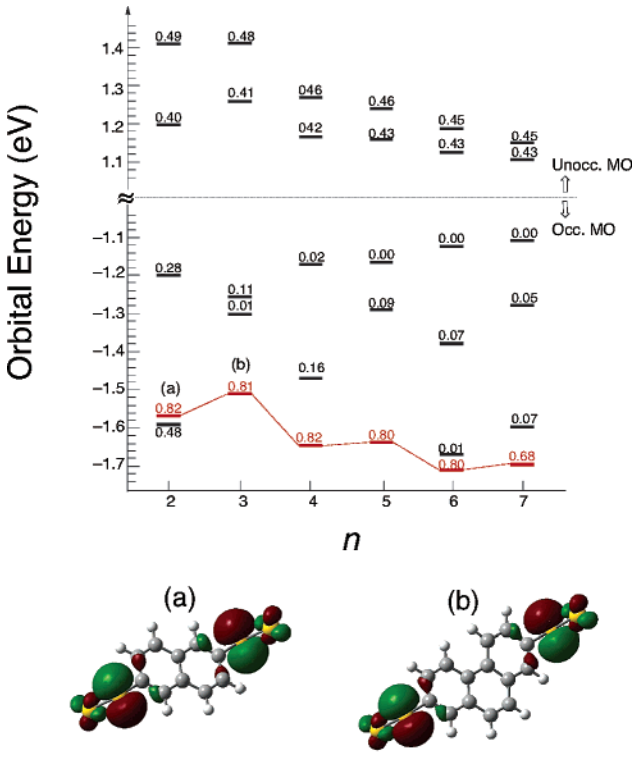

Figure 8. Orbital energy diagram of PPh(*n*)DTs for $n = 2$ to 7 in the vicinity of the Fermi level. The values included in the diagram indicate a population at a terminal sulfur atom in each MO. The MOs localized at the sulfur atoms (e.g., (a) and (b)) are depicted with red. The Fermi level is 0 eV.

feature of the conductance oscillation will be obtained in the HOMO-2 (the HOMO-3 for PPh(6)DTs and PPh(7)DT) or in the LUMO+2. Figure 8 shows an energy diagram of the frontier orbitals of PPh(*n*)DTs and the populations of a terminal sulfur atom ρ(S) in each MO. The LUMO+2 (not shown) is located far from the Fermi level (about 3 eV above E_F), and ρ(S)'s in the LUMO+2 are very small (0.01∼0.001). Thus, the LUMO+2 does not play an important role in the conductance. These MOs leading to the conductance oscillation are the HOMO-2 of PPh(*n*)DTs for $n = 3$ to 5; the HOMO-1 for $n = 2$ and the HOMO-3 for $n = 6$ and 7 also play a role in the conductance oscillation. These orbitals are depicted with red in Figure 8. The MOs affect the electrical conductance despite the large energy separations from the Fermi level because of their localized nature at the sulfur atoms. The orbital energies are lifted when *n* is odd, and therefore the contributions from the localized MOs for an odd-numbered *n* are larger than those for an even-numbered *n*, resulting in the conductance oscillation in PPh(*n*)DTs. In PA(*n*)DTs, we also obtained the localized nature in the HOMO-2 for $n = 3$ to 5 and in the HOMO-3 for $n = 6$ and 7. Although the energies of the localized orbitals of PA(*n*)DTs do not oscillate, the electron populations at the sulfur atoms in the MOs oscillate as follows: computed values for $n = 2$, 3, 4, 5, 6, and 7 are 0.82, 0.61, 0.68, 0.63, 0.66, and 0.61, respectively. The populations are relatively large when *n* is even, leading to the conductance oscillation of PA(*n*)DT. It is worthy to note that in other conjugated oligomers shown in Figure 6 neither orbital energies nor electron populations of the localized orbitals oscillate. We can reasonably conclude that the conductance oscillation is attributed to the oscillation of the orbital energies or electron populations of the localized orbitals.

5. Conclusions

We have calculated the electrical conductance of polyacene dithiolates (PA(*n*)DTs) and polyphenanthrene dithiolates (PPh(*n*)DTs) by using the Landauer formulation combined with density functional theory. Since this formulation is based on the Green functions expanded in terms of molecular orbitals (MOs), we can successfully derive important correlations between conductance and MOs in particular the frontier orbitals. When the number of benzene rings *n* included in the molecular wires is less than 7, the conductances of PA(*n*)DTs and PPh(*n*)DTs oscillate as a function of *n*. The conductance is enhanced in PA(*n*)DTs with even-numbered benzene rings, whereas it is enhanced in PPh(*n*)DTs with odd-numbered benzene rings. The conductance oscillation correlates with the oscillation of the orbital energies or electron populations at the terminal sulfur atoms. The damping factors in the exponential law of conductance for PA(2*m*)DT and PA(2*m*+1)DT are 0.089 and 0.032 Å^{-1}, respectively, and those for PPh(2*m*)DT and PPh(2*m*+1)DT are 0.371 and 0.406 Å^{-1}, respectively. In comparison with the damping factors of typical π conjugated oligomers (polyacetylene-DT, oligo(thiophene)-DT, oligo(*meso*-*meso*-linked zinc(II) porphyrin-butadiynylene)-DT, oligo(*p*-phenylethynylene)-DT, and oligo(*p*-phenylene)-DT), the damping factor of PA(2*m*+1)DT is the small limit and that of PPh(2*m*+1)DT is the large limit.

Althogh polyacene is attractive as a molecular wire because of its small damping factor, the synthesis of long acene oligomers is difficult at present. This situation may restrict the application of the unique electronic features of polyacene. It is

concluded from the conductance analysis of polyacene that one can obtain a small damping factor of conductance when the frontier orbitals of a series of molecular wires are close in energy to the Fermi level of electrodes. We see a similar electronic feature in the carbazole-based ladder polymers recently synthesized.[72] The HOMO levels of the ladder polymers are approximately −5.2 eV, which is close to the work function of gold (−5.31 eV). Thus, these synthesizable polymers can make a good molecular wire with a small damping factor.

Supporting Information Available: Figures S1 and S2 of optimized geometris of PA(*n*)DTs and PPh(*n*)DTs calculated with B3LYP/LANL2DZ. This material is available free of charge via the Internet at http://pubs.acs.org.

Acknowledgment. K.Y. acknowledges Grants-in-aid for Scientific Research from the Ministry of Education, Culture, Sports, Science and Technology of Japan (MEXT), Japan Society for the Promotion of Science (JSPS), Japan Science and Technology Cooperation (JST), the Murata Science Foundation, "Nanotechnology Support Project" of MEXT, and Kyushu University P & P 'Green Chemistry' for their support of this work. M.K. thanks JSPS for a graduate fellowship. Computations were in part carried out at the Computer Center of the Institute for Molecular Science.

JA031736+

(72) Dierschke, F.; Grimsdale, A. C.; Müllen, K. *Macromol. Chem. Phys.* **2004**, *205*, 1147.